Chemical Science

ROYAL SOCIETY OF CHEMISTRY

EDGE ARTICLE

View Article Online
View Journal | View Issue

Cite this: *Chem. Sci.*, 2023, **14**, 10602

All publication charges for this article have been paid for by the Royal Society of Chemistry

Received 3rd May 2023
Accepted 31st August 2023

DOI: 10.1039/d3sc02266h

rsc.li/chemical-science

Ruthenium(v) terminal arylimido corroles: isolation, spectroscopic characterization and reactivity†

Ka-Pan Shing, ‡[a] Lin Qin,‡[a] Liang-Liang Wu,[a] Jie-Sheng Huang *[a] and Chi-Ming Che *[ab]

Terminal Ru(v)–imido species are thought to be as reactive to group transfer reactions as their Ru(v)–oxo homologues, but are less studied. With the electron-rich corrole ligand, relatively stable and isolable Ru(v)–arylimido complexes [Ru(^{t}Bu–Cor)(NAr)] (H_3(^{t}Bu–Cor) = 5,15-diphenyl-10-(*p*-*tert*-butylphenyl) corrole, Ar = 2,4,6-$Me_3C_6H_2$ (Mes), 2,6-(^{i}Pr)$_2C_6H_3$ (Dipp), 2,4,6-(^{i}Pr)$_3C_6H_2$ (Tipp), and 3,5-$(CF_3)_2C_6H_3$ (BTF)) can be prepared from [Ru(^{t}Bu–Cor)]$_2$ under strongly reducing conditions. This type of Ru(v)–monoarylimido corrole complex with $S = \frac{1}{2}$ was characterized by high-resolution ESI mass spectrometry, X-band EPR, resonance Raman spectroscopy, magnetic susceptibility, and elemental analysis, together with computational studies. Under heating/light irradiation (xenon lamp) conditions, the complexes [Ru(^{t}Bu–Cor)(NAr)] (Ar = Mes, BTF) could undergo aziridination of styrenes and amination of benzylic C(sp^3)–H bonds with up to 90% product yields.

Introduction

Fe(v)- and Ru(v)–imido species are widely proposed but underexplored reactive intermediates in many Fe(iii) and Ru(iii)/Ru(iv)-catalysed C(sp^3)–H amination reactions.[1] Such reactive Fe(v)/Ru(v)–imido species can undergo atom-efficient functionalization of C–H bonds as their oxo-congeners (Fe(v)– and Ru(v)–oxo species),[2] but are unstable and short-lived in solution.[1b,3] Spectroscopic characterization and isolation of the Fe(v)/Ru(v)–imido complexes reactive towards hydrocarbons are essential for understanding their bonding, electronic structure, and reactivity. In the literature, although there are ample examples of well-characterized Ru(v)–oxo species,[2a,4] terminal Ru(v)–imido species are sparse.[5] Wilkinson and co-workers reported [^{n}Pr$_4$N][Ru(NCy){OCEt$_2$C(O)O}$_2$],[5d] but the reactivity of this isolable Ru–imido complex towards hydrocarbons has not been documented. Literature examples of spectroscopically characterized M(v)–imido complexes that can aziridinate alkenes and/or aminate C(sp^3)–H bonds, including Fe(v)–tosylimido species with the tetraamide ligand[1b] and Ru(v)–acylimido porphyrin[1e] complexes, are generated in solutions without isolation (Fig. 1a).

In order to obtain novel spectroscopically characterized M(v)–imido species reactive with hydrocarbons, and to improve the stability of such species, we attempted to focus on Ru(v) (considering the high reactivity of Ru(v)–acylimido porphyrin

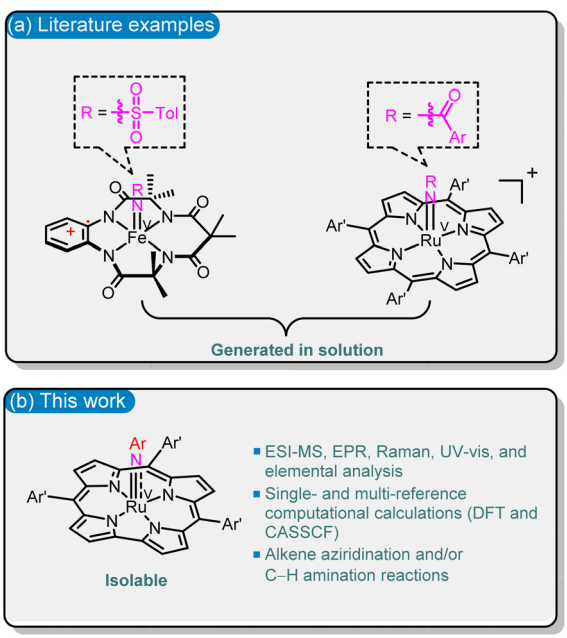

Fig. 1 Examples of (a) in the literature and (b) in this work for spectroscopically characterized M(v)–imido species that can undergo alkene aziridination and/or C–H amination reactions.

[a]*State Key Laboratory of Synthetic Chemistry, Department of Chemistry, The University of Hong Kong, Pokfulam Road, Hong Kong, China. E-mail: cmche@hku.hk*
[b]*HKU Shenzhen Institute of Research and Innovation, Shenzhen, China*

† Electronic supplementary information (ESI) available: Abbreviations, experimental procedures, characterization of compounds, computational details, Tables S1–S4, Fig. S1–S21, NMR spectra of compounds, and Cartesian coordinates from DFT calculations. CCDC 2214628. For ESI and crystallographic data in CIF or other electronic format see DOI: https://doi.org/10.1039/d3sc02266h

‡ These authors contributed equally.

species[1e]) and the use of the trianionic corrole (Cor) ligand; the latter was previously shown to stabilize the [M^{V}(Cor)(NAr)] (M = Cr, Mn, Re) species.[6] One hurdle to overcome is that most of the reported Ru corroles are dimers with strong Ru≡Ru triple bonds,[7] in contrast to the case of Ru porphyrins, where Ru_2(II,II) porphyrin dimers are highly sensitive to oxygen and are useful precursors for Ru–carbene, –oxo or –imido species.[8a,f] Here we report reductive activation of Ru_2(III,III) corrole dimers followed by reaction with aryl azides to give Ru(V)–arylimido (Ru^{V}(NAr)) complexes; the latter have been isolated and characterized by X-band EPR, resonance Raman (rR), HR-ESI-MS, UV-vis spectroscopy, elemental analysis, and/or DFT calculations. This type of Ru^{V}(NAr) complex can undergo alkene aziridination and C(sp^3)–H amination reactions, both of which have not been reported for [M^{V}(Cor)(NAr)] (M = Cr, Mn, Re).[6]

Results and discussion

Synthesis of Ru(V)–arylimido complexes

The Ru_2(III,III) corrole dimer [Ru(^{t}Bu–Cor)]$_2$ (**1**, Scheme 1) was prepared in 65% yield and characterized by NMR, UV-vis, HR-ESI-MS, cyclic voltammetry, elemental analysis and X-ray crystallography (Fig. S1 in the ESI†). We attempted to generate Ru(V)–imido species by reaction of **1** with aryl azide, but the dimer was quantitatively recovered. We envisage weakening the Ru≡Ru bond of **1** by reducing this complex. Reduction of **1** with excess potassium graphite (KC_8) in rigorously deoxygenated and dried THF, followed by overnight stirring at RT (Pyrex® Spinbar), afforded a species **2**, tentatively the reduced dimer {[Ru(^{t}Bu–Cor)]$_2$}$^{2-}$. The effective magnetic moment of **2** (*in situ* generated) was determined to be 2.81μ_B using the Evans method, which indicates that **2** is paramagnetic with two unpaired electrons ($S = 1$). This is in contrast to the dimer **1** ($S = 0$) and mononuclear Ru(II) corrole species, which are expected to be diamagnetic, similar to the Ru(II) porphyrin complexes [Ru(Por)(L)$_2$] (L = vacant or L = N_2, CH_3CN, THF, Et_2O).[8g] Based on its magnetic moment (2.81μ_B), complex **2** is likely to be a Ru_2(II,II) corrole dimer, whose electronic configuration ($S = 1$) is similar to that ($\sigma^2\pi^4(\delta_{nb})^4(\pi^*)^2$) of the Ru_2(II,II) porphyrin dimers reported by Collman and co-workers.[8d] Redox titration of **2** with [Cp_2Fe]PF_6 showed that *ca.* 2 equiv. of Cp_2Fe and 1 equiv. of **1** were generated. In a control experiment, **1** was not able to reduce [Cp_2Fe]PF_6 under the same reaction conditions. The UV-vis spectrum of **2** in THF shows pairwise Soret bands at 411 and 445 nm, which are red-shifted from that of **1** at 329 and 399 nm (Fig. S4 in the ESI†). A Ru_2(II,II) species, {[Ru(Cor)]$_2$}$^{2-}$, was previously proposed as the two-electron reduced product of [Ru(Cor)]$_2$ by Guilard and co-workers.[7b]

As shown in Scheme 1, treatment of **2** with aryl azides (ArN_3, Ar = Mes, Dipp, Tipp, BTF) afforded a set of Ru^{V}(NAr) complexes [Ru(^{t}Bu–Cor)(NAr)] (**3**); [Ru(^{t}Bu–Cor)(NBTF)] (**3d**) bearing the CF_3-substituted arylimido ligand is one of the rare examples of terminal imido complexes of late transition metals featuring strongly electron-withdrawing CF_3 substituents on their imido ligands.[9] The reactions using $MesN_3$ (for **3a**) and $BTFN_3$ (for **3d**) took only a few minutes, whereas the reactions with $DippN_3$ (for **3b**) and $TippN_3$ (for **3c**) bearing sterically more hindered aryl groups required stirring for 0.5 h at RT. Complexes **3** are likely formed *via* initial generation of [Ru^{IV}(^{t}Bu–Cor)(NAr)]$^-$ followed by disproportionation or one-electron oxidation. In the literature, Ru(IV)–oxo porphyrin was reported to undergo disproportionation;[8f,10] Fe(IV)–oxo porphyrins and Mn(IV)–oxo corroles have been reported to convert into their one-electron oxidized counterparts in solution.[11]

MALDI-TOF MS was used to monitor the reaction. In initial trials using "**1** + $MesN_3$" in refluxing benzene solution, a cluster peak attributable to **3a** was not observed. By using "**2** + $MesN_3$" (Fig. S6 in the ESI†), the ESI-MS spectrum of the reaction mixture showed a strong cluster peak at *m*/*z* 814.2479, which was attributed to the parent ion of [Ru(^{t}Bu–Cor)(NMes)] (**3a**, calcd for $C_{50}H_{42}N_5Ru$: 814.2492; Fig. S12 in the ESI†), giving the simulated isotope pattern that matches that observed experimentally. As expected, the peak is isotopically sensitive, with the isotope pattern changing upon using a 50% ^{15}N-enriched

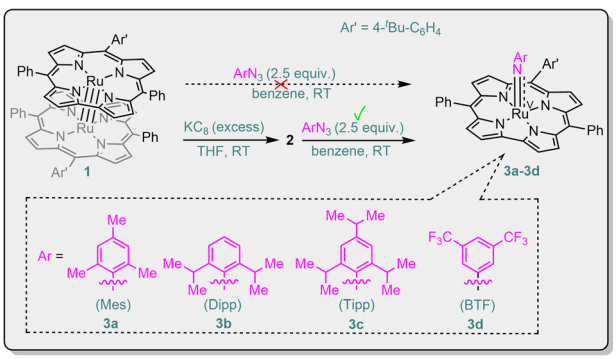

Scheme 1 Synthesis of Ru(V)–arylimido corrole complexes **3a–3d**.

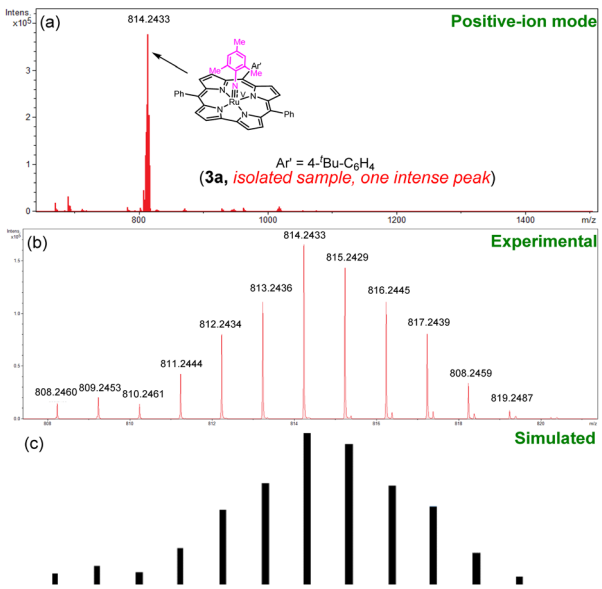

Fig. 2 (a) HR-ESI-MS (positive-ion mode) spectrum of [Ru(^{t}Bu–Cor)(NMes)] (**3a**). (b) Experimental isotope pattern of "[Ru(^{t}Bu–Cor)(^{14}NMes)]$^+$ + [Ru(^{t}Bu–Cor)(^{15}NMes)]$^+$" in a 1 : 1 ratio (50% ^{15}N enrichment). (c) Simulated pattern of (b).

sample (^{14,15}N–**3a**, prepared from ^{15}N–MesN$_3$; Fig. 2). Other Ru–arylimido complexes (**3b–3d**) have also been isolated and characterized by ESI-MS/MALDI-TOF MS. Complexes **3a–3d** were found to gradually decompose within 24 h even under an inert atmosphere and at low temperature (argon filled glove box, refrigerator pre-equilibrated at −35 °C), as evidenced by UV-vis spectroscopy and ESI-MS analysis. Attempts to obtain diffraction-quality crystals of these complexes for X-ray crystal structure determination were not successful.

EPR and electronic spectroscopy

After measuring their magnetic susceptibility (*ca.* 1.73μ_B using the Evans method), X-band EPR experiments were performed to elucidate the electronic structure of these Ru–arylimido corrole complexes **3**. An anisotropic EPR signal for **3a** (Fig. S16 in the ESI†) was found at frozen glass temperature (100 K, benzene). Upon treatment with 5 equiv. of PPh$_3$, this EPR signal diminished, and [Ru(^{t}Bu–Cor)(PPh$_3$)]$^+$ (Fig. S8 in the ESI,† *m*/*z* 943.4) and MesN=PPh$_3$ were found (Fig. S9 in the ESI;† *m*/*z* calcd: 396.1858, found: 396.1881; ^{31}P NMR in CDCl$_3$: −13.85 ppm).

The EPR spectrum of **3a** was simulated using the parameters of $g_x = 2.010$, $g_y = 2.005$, $g_z = 1.880$; A_x, A_y, $A_z = 53$, 14, 14 MHz (^{14}N). Simulation for the EPR spectrum of **3b** (Fig. S17 in the ESI†) was also carried out, by employing the *g* and *A* values of $g_x = 2.000$, $g_y = 1.980$, $g_z = 1.870$; A_x, A_y, $A_z = 50$, 14, 14 MHz (^{14}N). The EPR spectrum of **3c** (Fig. 3a) is similar to that of its structurally similar complex **3b** (*g* and *A* values for the simulated spectrum: same as those of **3b**), and the signal pattern is assigned to the superhyperfine coupling to the ^{14}N nucleus of the imido ligand, similar to that of Fe(v)–imido species.[12] For the 50% ^{15}N-enriched sample, ^{14,15}N–**3c** (prepared from ^{15}N–TippN$_3$), the corresponding EPR spectrum (Fig. 3b) shows a signal which can be reasonably fitted by summing the simulated spectra of **3c** and ^{15}N–**3c**, with a 1 : 1 ratio (Fig. 3b; ^{14}N: $I = 1$, ^{15}N: $I = \frac{1}{2}$). The EPR signals of **3a–3c** are characterized by g_{iso} ($g_x + g_y + g_z$)/3) values of 1.950–1.965, which can be assigned to Ru(v) complexes with $S = \frac{1}{2}$.[1e,2a] These g_{iso} values are similar to those of Ru(v)–acylimido and Ru(v)–oxo porphyrin complexes ($g_{iso} = 1.94$,[1e] 1.970 (ref. 2*a*)), but smaller than those commonly observed for Ru(III) complexes (g_{iso} = 2.1–2.3 (ref. 2*c* and 13)).

Complexes **3a–3d** each exhibit one Soret band (at 406–411 nm) in the UV-vis spectrum; like mononuclear [Ru^{VI}(Cor)(N)] complexes each complex also has one Soret band (at 417–419 nm),[7d] but unlike the Ru$_2$(III,III) dimer **1**, which exhibits two Soret bands (at 329 and 399 nm). In accord with the [Ru^V(Cor)(NAr)] formulation, the UV-vis spectra of **3a–3d** (Fig. S5 in the ESI†) do not show typical absorption bands of corrole π–cation radical (Cor$^{+\bullet}$) complexes (above 650 nm[14]). For example, a band at 676 nm was observed for [Mn^V(Cor$^{+\bullet}$)(N)],[15] the EPR spectrum of which (at 4 K) showed an isotropic radical signal, in contrast to the anisotropic EPR signals of **3a–3c**.

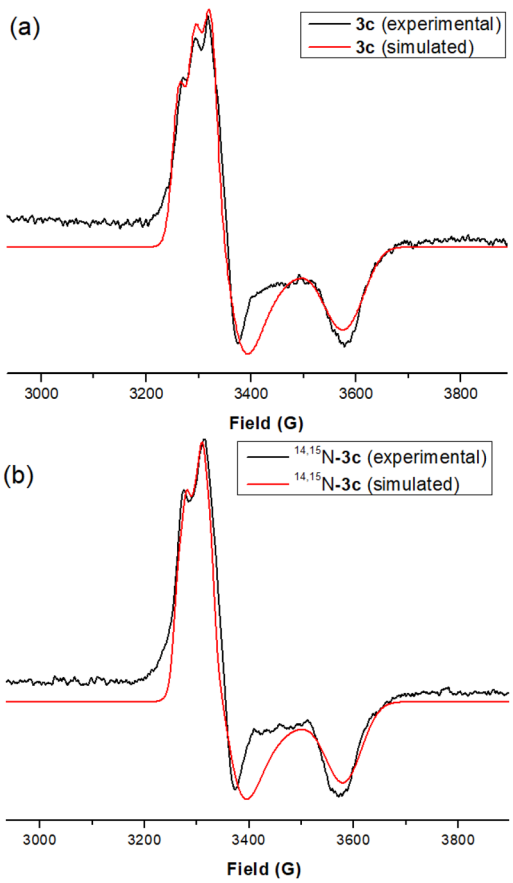

Fig. 3 X-band EPR spectra of isolated samples of (a) **3c** and (b) ^{14,15}N–**3c** recorded at 100 K.

Vibrational spectroscopy (IR and resonance Raman)

The vibrational spectra of **3a** and its 50% ^{15}N-enriched form ^{14,15}N–**3a** were recorded. No bands over 3200 cm^{-1} were found in the FTIR spectra (isolated solid samples, KBr pellets), in agreement with the absence of the amino/amido group in the complex. The ν(Ru≡^{14}NMes) band could possibly be obscured by an intense band of the coordinated corrole ligand at 1016 cm^{-1}; based on the FTIR spectroscopy, we tentatively assign the ν(Ru≡^{15}NMes) band of ^{14,15}N–**3a** at 972 cm^{-1}. To observe the ν(Ru≡^{14}NMes) and ν(Ru≡^{15}NMes) bands, we measured the resonance Raman (rR) spectra of **3a** and ^{14,15}N–**3a** (isolated samples dissolved in CH$_2$Cl$_2$). The rR spectrum of ^{14,15}N–**3a** (Fig. 4b, $\lambda_{excitation}$: 416 nm) shows pairwise bands (*ca.* 1 : 1 ratio due to 50% ^{15}N-enrichment) at ∼949 and 921 cm^{-1} with $\Delta\nu$ of ∼28 cm^{-1} agreeing with the value of 28 cm^{-1} estimated using Hooke's law. These two bands are assigned to ν(Ru≡^{14}NMes) and ν(Ru≡^{15}NMes), respectively, and the band at 921 cm^{-1} is absent in the rR spectrum of **3a** (Fig. 4a). By considering literature examples of rR studies on metal–arylimido (M(NAr), *e.g.*, Fe(NPh)[16]) complexes, other ^{15}N-isotopically sensitive bands within 820–1000 cm^{-1} may be associated with the coordinated arylimido ligand, where ^{15}N-labelling resulted in a downshift of the bands involving M–N$_{imido}$ and aryl groups.

N-group transfer reactivities

Complex **3a**, which has a moderately hindered mesitylimido ligand with electron-donating Me groups, was reacted with styrene at 85 °C for 24 h (entry 1 in Table 1) to give 1-mesityl-2-

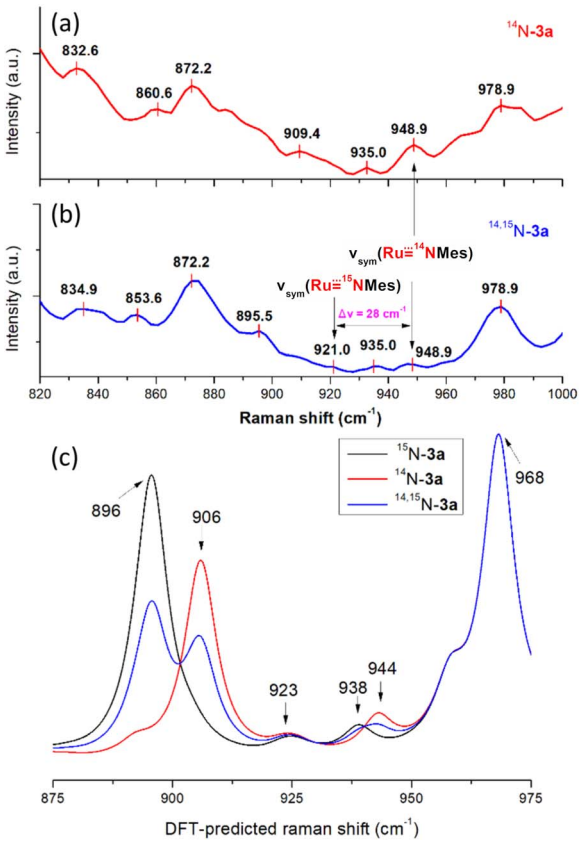

Fig. 4 rR spectra of the isolated samples (dissolved in dry CH_2Cl_2) of (a) **3a** and (b) ^{14,15}N–**3a**. (c) DFT-calculated Raman spectra of **3a**, ^{15}N–**3a** and ^{14,15}N–**3a**.

phenylaziridine in 69% yield. Under the same conditions, the reaction of **3d** bearing the 3,5-bis(trifluoromethyl)phenylimido ligand with styrene gave the aziridine product in much higher yield (90%; entry 2 in Table 1). This is attributed to the lower steric hindrance and higher electrophilicity of the 3,5-bis(trifluoromethyl)phenylimido ligand compared with the mesitylimido ligand. Reactive M(NAr) complexes with Ar = 3,5-bis(trifluoromethyl)phenyl (BTF) or other groups (*e.g.* C_6F_5, CF_3–C_6F_4 and NO_2–C_6H_4) with electron-withdrawing substituents are reactive intermediates involved in metal-catalysed N-group transfer reactions using the corresponding aryl azides.[17] Reaction of **3d** with *cis*-stilbene at 85 °C for 24 h gave *trans*-aziridine in 62% yield; *cis*-aziridine was not detected (entry 3 in Table 1). The reaction of 1,1-diphenylethylene with **3d** gave diphenylaziridine in lower yield (49%, entry 4 in Table 1). This is attributed to the steric effect, as α-methylstyrene (which is sterically less hindered than 1,1-diphenylethylene) was found to react with **3d** to give methylphenylaziridine in higher yield (76%, entry 5 in Table 1). **3d** was reacted with excess cyclohexene at 85 °C for 24 h, and neither aziridination of the C=C bond nor amination of the allylic C(sp^3)–H bond was observed.

We then examined the amination of benzylic C(sp^3)–H bonds with **3d**. Treatment of **3d** with excess isochroman gave the amination product in <1% yield, whereas the reaction of indane and phthalane with **3d** gave the amination product in 12% and

Table 1 Stoichiometric reaction of Ru(v)–arylimido corrole complexes with alkenes/C–H bonds[a]

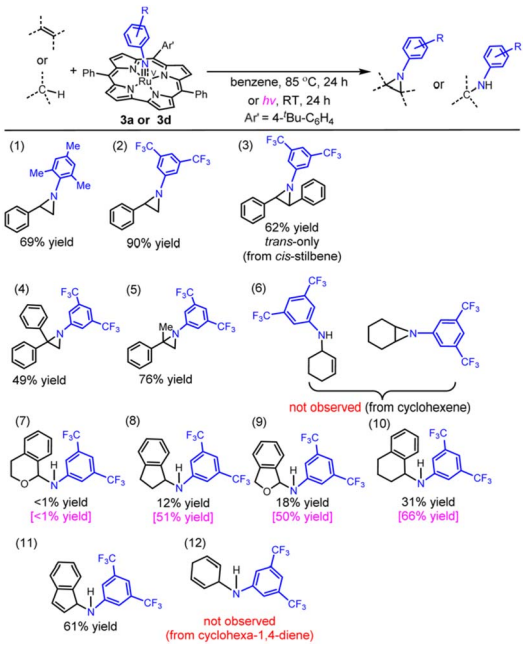

[a] Ru(v)–arylimido complex (5.50 μmol) and the substrate (1.65 mmol) in benzene (1 mL); the product yields under UV-vis irradiation are presented in pink colour whereas the black ones refer to the yields obtained at 85 °C.

18% yields, respectively (entries 7–9 in Table 1; 85 °C for 24 h). The reaction of **3d** with tetralin gave the amination product in 31% yield (entry 10 in Table 1; 29% yield for a 1 h reaction). Complex **3d** exhibited a relatively high reactivity towards indene (61% yield of the amine product; entry 11 in Table 1). We found that light irradiation at RT (xenon lamp) promoted the **3d**-mediated amination of indane, phthalane and tetralin as revealed by the higher product yields obtained (50–66% yield; entries 8–10 in Table 1). Indane and phthalane gave higher yield of the amination product than isochroman, which may be related to the statistical factor because isochroman has a smaller number of equivalent C–H bonds for the amination. In the amination of tetralin and indane by **3d**, the product yield was found to decrease with increasing dissociation energy of the reactive C–H bond (*cf.* 82.9 and 85.3 kcal mol^{-1} for tetralin and indane, respectively[18]).

Catalytic N-group transfer reactions were examined using Ru corrole complexes **1** and **2** as catalysts. For the **1**-catalysed reaction of styrene with aryl azide $BTFN_3$ in benzene at 85 °C, the aziridination product was obtained in 5% yield. Upon changing the catalyst to **2**, a much higher product yield of 46% was achieved (entries 1 and 2 in Table 2). Complex **2** also catalysed the aziridination of *para*-substituted styrenes to aziridines in 38–54% yields (entries 3–6 in Table 2). Using *cis*-stilbene as the substrate, the reaction afforded *trans*-aziridine as the major product (*trans*/*cis* ratio: 2.9 : 1.0, 48% yield, entry 8 in Table 2).

Table 2 Catalytic aziridination of alkenes using a Ru corrole complex as the catalyst[a]

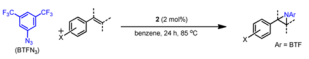

Entry	Substrate	Product	Yield
1[b]			5%
2			46%
3			38%
4			49%
5			43%
6			54%
7[c]			7% (*trans*/*cis* = 0.2 : 1.0)
8			48% (*trans*/*cis* = 2.9 : 1.0)

[a] Reaction conditions: **2**/ArN_3/styrene = 1 : 50 : 250; yields were determined by ^{1}H NMR analysis. [b] Using **1** as the catalyst. [c] No metal catalyst was used.

Regarding the mechanism of the **3d**-mediated aziridination of alkenes, we conceive that the aziridination proceeds in a stepwise manner due to the formation of *trans*-aziridine from *cis*-stilbene (entry 3 in Table 1). For the aziridination of *para*-substituted styrenes by **3d**, the plot of $\log(k_{rel})$ against σ_{mb} and $\sigma^{\bullet}_{JJ}$, using a dual parameter equation developed by Jiang and co-workers,[19] shows a good linearity ($R^2 = 0.9979$) featuring $\rho_{mb} = -0.54$ and $\rho^{\bullet}_{JJ} = 0.43$ (Fig. 5), with the linearity being better than that for the plot of $\log(k_{rel})$ against σ^+ (Fig. S15 in the ESI;† $R^2 = 0.9356$). This is consistent with a stepwise mechanism in which a carboradical is involved. A positive value of $\rho^{\bullet}_{JJ}$ indicates the spin density of the radical centre delocalized by the *para*-substituent, while a negative value of ρ_{mb} supports electrophilic attack of styrene by **3d**.

Furthermore, we examined the deuterium kinetic isotope effect (KIE) for **3d**-mediated C(sp^3)–H amination by using equimolar and excess of tetralin and d_4-tetralin. The k_H/k_D value determined for such amination by **3d** at 383 K is 4.0(2), comparable to that reported for the C(sp^3)–H amination of ethylbenzene by [Ru^{VI}(TMP)($NNs)_2$] ($k_H/k_D = 4.8$) at 298 K.[20]

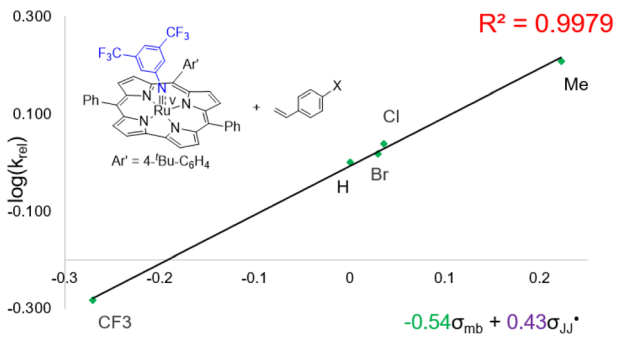

Fig. 5 Hammett correlation for the aziridination of *para*-substituted styrenes mediated by **3d** using a dual-parameter method (σ_{mb} and $\sigma^{\bullet}_{JJ}$).

We propose that the C–H amination mediated by **3d** involves a stepwise mechanism similar to that for the [Ru^{VI}(TMP)($NNs)_2$]-mediated amination,[20] characterized by H atom abstraction followed by radical rebound.

Computational studies

We first calculated the Raman spectrum of **3a** and ^{14,15}N–**3a** to check the accuracy and reliability of the computational studies. The calculated energy bands of $\nu\left(Ru{=}{=}{=}^{14}N\right)$ and $\nu\left(Ru{=}{=}{=}^{15}N\right)$ are located at 944 and 923 cm^{-1}, respectively (Fig. 4c), which are consistent with the respective experimental values (~949 and 921 cm^{-1}). By converting the Raman shifts to bond distances, **3a** has a calculated Ru–N_{imido} distance of 1.756 Å. The calculated Ru–N_{imido} distances for **3b** and **3d** are 1.779 and 1.763 Å, respectively. In terms of the Wiberg bond index (WBI), **3a**, **3b** and **3d** have predicted Ru–N_{imido} bond orders of 2.05, 1.96 and 2.04, respectively, indicating a multiple bond character. This is in contrast to the cobalt complex with the imidyl ligand $NDipp^{+\bullet}$, which is characterized by a calculated single Co–N_{imidyl} bond character (WBI ≈ 1.0).[21]

Similar to the previously reported Ru(v)–oxo porphyrin,[2a] both **3a** and **3b** adopt an $S = 1/2$ ground state with $(d_{xy})^2(d_{xz},d_{yz})^1(d_{z^2})^0(d_{x^2-y^2})^0$ configuration. In both species, the singly occupied molecular orbital (SOMO) corresponds to d_π, while the π orbitals of the corrole ligand are *ca.* 0.4–0.5 eV lower than the SOMO, indicating that the corrole ligand is not redox-active (Fig. S18 in the ESI†). We calculated *g* values for **3a** by DFT calculations; the calculated results ($g = 2.010, 2.000, 1.890$) are in good agreement with the values based on the experimental EPR spectrum ($g = 2.010, 2.005, 1.880$) (Table S3 in the ESI†). By DFT calculations, the % spin density on Ru/N_{imido} atom (% $SD_{Ru/N}$) of **3a**, **3b**, and **3d** is 44/27, 35/36, and 53/19, respectively, and that on the coordinated arylimido ligand (% SD_{NAr}) of **3a**/**3b**/**3d** is 40/54/26 (Fig. 6).

The decrease of spin density on the arylimido ligand (% SD_{NAr}) along the series **3b** > **3a** > **3d** is in line with the decrease of the Ru–N_{imido}–C_{Ar} angle along the same series (160°, 146° and 138° for the DFT-optimized structures of **3b**, **3a**, and **3d**, respectively; Fig. 6). The arylimido ligand of **3b** bears bulky 2,6-substituents (^{i}Pr) and adopts a basically linear coordination mode, which minimizes steric conflicts between these substituents and the corrole ligand. Complex **3a** has less bulky 2,6-substituents (Me); its arylimido ligand can accommodate a relatively bent coordination mode.[22] A more bent coordination mode of the arylimido ligand corresponds to **3d** which possesses no 2,6-substituents and bears electron-withdrawing 3,5-CF_3 groups, like the case of [Ru^{VI}(TPP)($NBTF)_2$] (Ru–N_{imido}–C_{Ar} angles: 139.8(3)° and 143.7(4)°).[23] The bending of the Ru–N_{imido}–C_{Ar} moiety would reduce spin delocalization along the *z*-axis (and into the aryl ring), thus decreasing the spin density on the arylimido group.

As the spin density on N_{imido} is the highest in **3b** among **3a**, **3b**, and **3d**, we performed multi-reference calculations for **3b** using the complete active space self-consistent field (CASSCF) method to check if Ru(iv)-imidyl character is involved.[17a,24] The

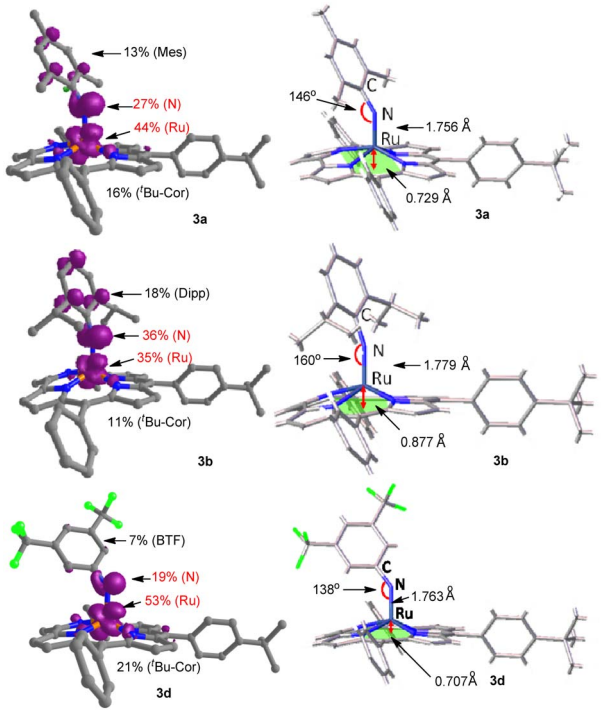

Fig. 6 DFT-optimized spin density distributions (contour value: 0.005), bond angles, bond distances and out-of-plane deviations.

calculation results revealed that **3b** can be described as "85.9% of [Ru^{V}(^{t}Bu–Cor)(NDipp)] + 3.6% of [Ru^{IV}(^{t}Bu–Cor)(NDipp$^{+\bullet}$)]" (Fig. 7). For the Ru–N_{imido} bond of **3b**, a calculated bond order of 2.04 was obtained by considering the matrix of atomic orbital coefficients for all relevant molecular orbitals. Based on the occupation numbers of orbitals within the active space, the calculated Ru–N_{imido} bond order is 2.27, close to the formal bond order of 2.5 with $\sigma^2\pi^4(\pi^*)^1$ configuration. The spin population obtained from the CASSCF calculation is 0.55 on Ru and 0.35 on N_{imido} (Fig. S19 in the ESI†), indicating that **3b** has a doublet ground state with the unpaired electron mainly residing on the Ru centre. This provides support for the formulation of **3b**, and also **3a** and **3d**, as a formal Ru(v)–arylimido corrole species bearing considerable spin density on N_{imido}.

We compared the DFT calculation results for the Ru(NAr) complexes having an $S = 1/2$ ground state, including % spin density on Ru/NAr (% $SD_{Ru/NAr}$) and the Ru–N_{NAr} distance (Table S4 in the ESI†). The % $SD_{Ru/NAr}$ of [(SiP^{iPr}_3)Ru(N–*p*-$CF_3C_6H_4$)][25a] and [Ru(PNP)(NPh)] (PNP = [($^{t}Bu_2PCH_2SiMe_2$)$_2$N]$^-$)[25b] with different types of monoanionic supporting ligands is 40/54 and 30/68, respectively. In the case of complexes **3** with the same trianionic ^{t}Bu–Cor supporting ligand, a direct comparison of % $SD_{Ru/NAr}$ among various Ar groups can be made (**3a**: 44/40, **3b**: 35/54, and **3d**: 53/26); the % SD_{NAr} decreases along the **3b** > **3a** > **3d** series as discussed above. The Ru–N_{NAr} distances in [(SiP^{iPr}_3)Ru(N–*p*-$CF_3C_6H_4$)] and [Ru(PNP)(NPh)] (*ca.* 1.81–1.87 Å) are longer than in complexes **3** (*ca.* 1.76–1.78 Å).

The electronic structure of the Ru(v)–arylimido complex **3b** calculated by CASSCF is different from that of the Fe(v)–

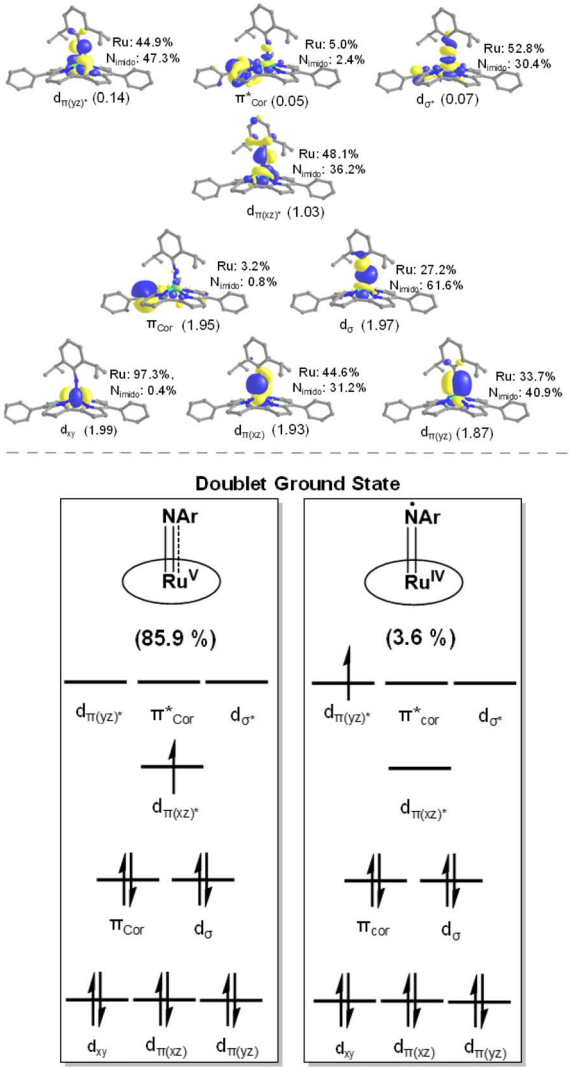

Fig. 7 Multi-configurational calculations (CASSCF method) using an active space of 11-electron, 9-orbital, *i.e.*, CASSCF(11,9) to depict leading configurations of the doublet ground state of **3b**. The remaining configurations each occupy <1% of the ground state. The natural orbitals associated with the assignment, occupation numbers (in parentheses) and atomic orbital contributions are shown in the upper panel (not according to relative energies).

tosylimido species [Fe^{V}(TAML)(NTs)]$^-$ calculated by DFT;[1b,26] the properties of the M–N_{imido} π- and π*-bonding of these two complexes are different. For **3b** with an essentially linear M–N_{imido}–C_{Ar} moiety (bond angle: 160°), two sets of π and π* orbitals between M-$d_{xz/yz}$ and N-$p_{x/y}$ are involved, reminiscent of the corresponding CASSCF calculation results for other M(NAr) complexes with linear M–N_{imido}–C_{Ar} moieties.[27] However, for [Fe^{V}(TAML)(NTs)]$^-$ having a bent Fe–N_{imido}–S_{Ts} moiety (bond angle: 126° (ref. 1*b*)), only the π and π* orbitals between M-d_{yz} and N-p_y are involved, and the M-d_{xz} is non-bonding.[26]

DFT calculations were also carried out for the aziridination of *cis*-stilbene by **3d**, which was experimentally found to favour the formation of the *trans*-aziridine product. The calculated reaction profile (Fig. S20 in the ESI†) involving the formation of a carboradical intermediate (**Int-*trans*** and **Int-*cis*** for *trans*- and

cis-configuration, respectively) is consistent with the proposed stepwise mechanism. The ring-closure barrier for **Int-*trans*** and **Int-*cis*** is 14.1 and 13.3 kcal mol^{-1}, respectively, both of which are larger than the barrier of 10.7 kcal mol^{-1} required for isomerization of **Int-*cis*** to the thermodynamically more favourable **Int-*trans*** by rotation about the C_{Ph}–C_{Ph} bond, allowing such rotation to take place prior to the ring closure, giving *trans*-aziridine as the major product.[28]

Conclusions

The electron-rich trianionic corrole ligand ^{t}Bu–Cor is capable of stabilizing reactive M(v)–imido species, enabling the isolation and spectroscopic characterization of reactive Ru(v)–arylimido complexes capable of undergoing N-group transfer with hydrocarbons. The relatively stable Ru(v)–arylimido corroles [Ru(^{t}Bu–Cor)(NAr)] (**3**) isolated in this work have been characterized by X-band EPR, rR, ESI or MALDI-TOF MS, and elemental analysis. Their electronic structures were examined by single- (DFT) and multi-reference (CASSCF) computational studies. Complexes **3** could aziridinate alkenes and aminate benzylic C(sp^3)–H bonds *via* a stepwise mechanism under heating/irradiation conditions, with product yields of up to 90% and 66%, respectively. The results of this work provide useful insights into the development of alkene and C(sp^3)–H bond functionalization *via* reactive Ru(v)–arylimido intermediates.

Author contributions

CMC conceived the idea and directed the project. KPS and LQ performed the experiments. LLW carried out the computational studies. KPS, LQ, JSH and CMC analysed the data. KPS, JSH and CMC wrote the manuscript.

Conflicts of interest

There are no conflicts to declare.

Acknowledgements

This work was supported by the Hong Kong Research Grants Council (HKU 17304019) and Basic Research Program-Shenzhen Fund (JCYJ20180508162429786). We thank Dr Xiao-Yong Chang for assistance in X-ray crystal structure determination of complex **1**.

Notes and references

1 (*a*) K.-P. Shing, Y. Liu, B. Cao, X.-Y. Chang, T. You and C.-M. Che, *Angew. Chem., Int. Ed.*, 2018, **57**, 11947; (*b*) S. Hong, K. D. Sutherlin, A. K. Vardhaman, J. J. Yan, S. Park, Y.-M. Lee, S. Jang, X. Lu, T. Ohta, T. Ogura, E. I. Solomon and W. Nam, *J. Am. Chem. Soc.*, 2017, **139**, 8800; (*c*) Y.-D. Du, C.-Y. Zhou, W.-P. To, H.-X. Wang and C.-M. Che, *Chem. Sci.*, 2020, **11**, 4680; (*d*) W. Xiao, J. Wei, C.-Y. Zhou and C.-M. Che, *Chem. Commun.*, 2013, **49**, 4619; (*e*) D.-Y. Hong, Y. Liu, L. Wu, V. K.-Y. Lo, P. H. Toy, S.-M. Law, J.-S. Huang and C.-M. Che, *Angew. Chem., Int. Ed.*, 2021, **133**, 18619; (*f*) R. Vyas, G.-Y. Gao, J. D. Harden and X. P. Zhang, *Org. Lett.*, 2004, **6**, 1907; (*g*) Y. Liu, G.-Q. Chen, C.-W. Tse, X. Guan, Z.-J. Xu, J.-S. Huang and C.-M. Che, *Chem.–Asian J.*, 2015, **10**, 100.

2 (*a*) K.-P. Shing, B. Cao, Y. Liu, H. K. Lee, M.-D. Li, D. L. Phillips, X.-Y. Chang and C.-M. Che, *J. Am. Chem. Soc.*, 2018, **140**, 7032; (*b*) F. T. de Oliveira, A. Chanda, D. Banerjee, X. Shan, S. Mondal, L. Que Jr, E. L. Bominaar, E. Münck and T. J. Collins, *Science*, 2007, **315**, 835; (*c*) C. Wang, K. V. Shalyaev, M. Bonchio, T. Carofiglio and J. T. Groves, *Inorg. Chem.*, 2006, **45**, 4769; (*d*) E. Vanover, Y. Huang, L. Xu, M. Newcomb and R. Zhang, *Org. Lett.*, 2010, **12**, 2246; (*e*) O. Y. Lyakin, A. M. Zima, N. V. Tkachenko, K. P. Bryliakov and E. P. Talsi, *ACS Catal.*, 2018, **8**, 5255.

3 (*a*) S. Hong, X. Lu, Y.-M. Lee, M. S. Seo, T. Ohta, T. Ogura, M. Clémancey, P. Maldivi, J.-M. Latour, R. Sarangi and W. Nam, *J. Am. Chem. Soc.*, 2017, **139**, 14372; (*b*) K. M. Van Heuvelen, A. T. Fiedler, X. Shan, R. F. De Hont, K. K. Meier, E. L. Bominaar, E. Münck and L. Que Jr, *Proc. Natl. Acad. Sci. U.S.A.*, 2012, **109**, 11933.

4 (*a*) A. C. Dengel, W. P. Griffith, C. A. O'Mahoney and D. J. Williams, *J. Chem. Soc., Chem. Commun.*, 1989, 1720; (*b*) C.-M. Che, V. W.-W. Yam and T. C. W. Mak, *J. Am. Chem. Soc.*, 1990, **112**, 2284; (*c*) N. L. P. Fackler, S. Zhang and T. V. O'Halloran, *J. Am. Chem. Soc.*, 1996, **118**, 481; (*d*) A. C. Dengel and W. P. Griffith, *Inorg. Chem.*, 1991, **30**, 869; (*e*) J. J. Concepcion, J. W. Jurss, M. K. Brennaman, P. G. Hoertz, A. O. T. Patrocinio, N. Y. M. Iha, J. L. Templeton and T. J. Meyer, *Acc. Chem. Res.*, 2009, **42**, 1954; (*f*) C.-M. Che, K.-Y. Wong and T. C. W. Mak, *J. Chem. Soc., Chem. Commun.*, 1985, 988; (*g*) L. Duan, F. Bozoglian, S. Mandal, B. Stewart, T. Privalov, A. Llobet and L. Sun, *Nat. Chem.*, 2012, **4**, 418; (*h*) Y. Liu, S.-M. Ng, S.-M. Yiu, W. W. Y. Lam, X.-G. Wei, K.-C. Lau and T.-C. Lau, *Angew. Chem., Int. Ed.*, 2014, **53**, 14468; (*i*) D. Lebedev, Y. Pineda-Galvan, Y. Tokimaru, A. Fedorov, N. Kaeffer, C. Copéret and Y. Pushkar, *J. Am. Chem. Soc.*, 2018, **140**, 451; (*j*) D. Moonshiram, I. Alperovich, J. J. Concepcion, T. J. Meyer and Y. Pushkar, *Proc. Natl. Acad. Sci. U.S.A.*, 2013, **110**, 3765; (*k*) C.-M. Che and K.-Y. Wong, *J. Chem. Soc., Chem. Commun.*, 1986, 229.

5 (*a*) W.-H. Leung, T. S. M. Hun, H.-w. Hou and K.-Y. Wong, *J. Chem. Soc., Dalton Trans.*, 1997, 237; (*b*) T. Ishizuka, T. Kogawa, M. Makino, Y. Shiota, K. Ohara, H. Kotani, S. Nozawa, S.-i. Adachi, K. Yamaguchi, K. Yoshizawa and T. Kojima, *Inorg. Chem.*, 2019, **58**, 12815; (*c*) R. P. Tooze, G. Wilkinson, M. Motevalli and M. B. Hursthouse, *J. Chem. Soc., Dalton Trans.*, 1986, 2711; (*d*) C. Redshaw, W. Clegg and G. Wilkinson, *J. Chem. Soc., Dalton Trans.*, 1992, 2059.

6 (*a*) A. B. Alemayehu, S. J. Teat, S. M. Borisov and A. Ghosh, *Inorg. Chem.*, 2020, **59**, 6382; (*b*) R. A. Eikey, S. I. Khan and M. M. Abu-Omar, *Angew. Chem., Int. Ed.*, 2002, **41**, 3591; (*c*) N. Y. Edwards, R. A. Eikey, M. I. Loring and M. M. Abu-Omar, *Inorg. Chem.*, 2005, **44**, 3700.

7 (*a*) F. Jérôme, B. Billier, J.-M. Barbe, E. Espinosa, S. Dahaoui, C. Lecomte and R. Guilard, *Angew. Chem., Int. Ed.*, 2000, **39**, 4051; (*b*) K. M. Kadish, F. Burdet, F. Jérôme, J.-M. Barbe, Z. Ou, J. Shao and R. Guilard, *J. Organomet. Chem.*, 2002, **652**, 69; (*c*) L. Simhovich, L. Luobeznova, I. Goldberg and Z. Gross, *Chem.–Eur. J.*, 2003, **9**, 201; (*d*) A. B. Alemayehu, H. Vazquez-Lima, K. J. Gagnon and A. Ghosh, *Inorg. Chem.*, 2017, **56**, 5285.

8 (*a*) P. J. Brothers and J. P. Collman, *Acc. Chem. Res.*, 1986, **19**, 209; (*b*) J. P. Collman, P. J. Brothers, L. McElwee-White, E. Rose and L. J. Wright, *J. Am. Chem. Soc.*, 1985, **107**, 4570; (*c*) J. A. Smieja, K. Shirzad, M. Roy, K. Kittilstved and B. Twamley, *Inorg. Chim. Acta*, 2002, **335**, 141; (*d*) J. P. Collman, C. E. Barnes, P. N. Swepston and J. A. Ibers, *J. Am. Chem. Soc.*, 1984, **106**, 3500; (*e*) J. P. Collman, E. Rose and G. D. Venburg, *J. Chem. Soc., Chem. Commun.*, 1993, 934; (*f*) J. T. Groves and K.-H. Ahn, *Inorg. Chem.*, 1987, **26**, 3831; (*g*) M. J. Camenzind, B. R. James and D. Dolphin, *J. Chem. Soc., Chem. Commun.*, 1986, 1137.

9 (*a*) S. Fantauzzi, E. Gallo, A. Caselli, F. Ragaini, N. Casati, P. Macchi and S. Cenini, *Chem. Commun.*, 2009, 3952; (*b*) Q. Liu, L. Long, P. Ma, Y. Ma, X. Leng, J. Xiao, H. Chen and L. Deng, *Cell Rep. Phys. Sci.*, 2021, **2**, 100454; (*c*) J. Xiong, Q. Liu, B. Lavina, M. Y. Hu, J. Zhao, E. E. Alp, L. Deng, S. Ye and Y. Guo, *Chem. Sci.*, 2023, **14**, 2808.

10 (*a*) W.-H. Leung and C.-M. Che, *J. Am. Chem. Soc.*, 1989, **111**, 8812; (*b*) M. B. Ezhova and B. R. James, in *Advances in Catalytic Activation of Dioxygen by Metal Complexes*, ed. L. I. Simándi, Springer, Boston, 2003, vol. 26, ch. 1, p. 1.

11 (*a*) R. Zhang, J. H. Horner and M. Newcomb, *J. Am. Chem. Soc.*, 2005, **127**, 6573; (*b*) J. T. Groves, Z. Gross and M. K. Stern, *Inorg. Chem.*, 1994, **33**, 5065.

12 M. Keilwerth, W. Mao, S. A. V. Jannuzzi, L. Grunwald, F. W. Heinemann, A. Scheurer, J. Sutter, S. DeBeer, D. Munz and K. Meyer, *J. Am. Chem. Soc.*, 2023, **145**, 873.

13 (*a*) P. Singh, A. K. Das, B. Sarkar, M. Niemeyer, F. Roncaroli, J. A. Olabe, J. Fiedler, S. Záliš and W. Kaim, *Inorg. Chem.*, 2008, **47**, 7106; (*b*) J. T. Groves, M. Bonchio, T. Carofiglio and K. Shalyaev, *J. Am. Chem. Soc.*, 1996, **118**, 8961; (*c*) B. R. James, D. Dolphin, T. W. Leung, F. W. B. Einstein and A. C. Willis, *Can. J. Chem.*, 1984, **62**, 1238; (*d*) M. M. Taqui Khan, D. Srinivas, R. I. Kureshy and N. H. Khan, *Inorg. Chem.*, 1990, **29**, 2320.

14 (*a*) R. Zhang and M. Newcomb, *Acc. Chem. Res.*, 2008, **41**, 468; (*b*) L. Simkhovich, A. Mahammed, I. Goldberg and Z. Gross, *Chem.–Eur. J.*, 2001, **7**, 1041; (*c*) D. N. Harischandra, R. Zhang and M. Newcomb, *J. Am. Chem. Soc.*, 2005, **127**, 13776.

15 H. Shi, R. Liang, D. L. Phillips, H. K. Lee, W.-L. Man, K.-C. Lau, S.-M. Yiu and T.-C. Lau, *J. Am. Chem. Soc.*, 2022, **144**, 7588.

16 M. P. Mehn, S. D. Brown, D. M. Jenkins, J. C. Peters and L. Que Jr, *Inorg. Chem.*, 2006, **45**, 7417.

17 (*a*) K. M. Carsch, I. M. DiMucci, D. A. Iovan, A. Li, S.-L. Zheng, C. J. Titus, S. J. Lee, K. D. Irwin, D. Nordlund, K. M. Lancaster and T. A. Betley, *Science*, 2019, **365**, 1138; (*b*) K.-H. Chan, X. Guan, V. K.-Y. Lo and C.-M. Che, *Angew. Chem., Int. Ed.*, 2014, **53**, 2982; (*c*) Y.-D. Du, Z.-J. Xu, C.-Y. Zhou and C.-M. Che, *Org. Lett.*, 2019, **21**, 895; (*d*) J. Wei, W. Xiao, C.-Y. Zhou and C.-M. Che, *Chem. Commun.*, 2014, **50**, 3373; (*e*) L.-M. Jin, X. Xu, H. Lu, X. Cui, L. Wojtas and X. P. Zhang, *Angew. Chem., Int. Ed.*, 2013, **52**, 5309; (*f*) F. Ragaini, A. Penoni, E. Gallo, S. Tollari, C. L. Gotti, M. Lapadula, E. Mangioni and S. Cenini, *Chem.–Eur. J.*, 2003, **9**, 249.

18 X.-S. Xue, P. Ji, B. Zhou and J.-P. Cheng, *Chem. Rev.*, 2017, **117**, 8622.

19 X.-K. Jiang, *Acc. Chem. Res.*, 1997, **30**, 283.

20 S. K.-Y. Leung, W.-M. Tsui, J.-S. Huang, C.-M. Che, J.-L. Liang and N. Zhu, *J. Am. Chem. Soc.*, 2005, **127**, 16629.

21 A. Reckziegel, M. Kour, B. Battistella, S. Mebs, K. Beuthert, R. Berger and C. G. Werncke, *Angew. Chem., Int. Ed.*, 2021, **60**, 15376.

22 (*a*) P. Barrie, T. A. Coffey, G. D. Forster and G. Hogarth, *J. Chem. Soc., Dalton Trans.*, 1999, 4519; (*b*) M. J. Zdilla and M. M. Abu-Omar, *J. Am. Chem. Soc.*, 2006, **128**, 16971; (*c*) V. C. Gibson, C. Redshaw, W. Clegg and M. R. J. Elsegood, *Polyhedron*, 2007, **26**, 3161.

23 D. Intrieri, A. Caselli, F. Ragaini, P. Macchi, N. Casati and E. Gallo, *Eur. J. Inorg. Chem.*, 2012, 569.

24 N. P. van Leest, M. A. Tepaske, J.-P. H. Oudsen, B. Venderbosch, N. R. Rietdijk, M. A. Siegler, M. Tromp, J. I. van der Vlugt and B. de Bruin, *J. Am. Chem. Soc.*, 2020, **142**, 552.

25 (*a*) A. Takaoka, L. C. H. Gerber and J. C. Peters, *Angew. Chem., Int. Ed.*, 2010, **49**, 4088; (*b*) A. N. Walstrom, B. C. Fullmer, H. Fan, M. Pink, D. T. Buschhorn and K. G. Caulton, *Inorg. Chem.*, 2008, **47**, 9002.

26 M. Mahajan and B. Mondal, *Inorg. Chem.*, 2023, **62**, 5810.

27 For recent examples, see: (*a*) Y. Park, S. P. Semproni, H. Zhong and P. J. Chirik, *Angew. Chem., Int. Ed.*, 2021, **60**, 14376; (*b*) W. Mao, Z. Zhang, D. Fehn, S. A. V. Jannuzzi, F. W. Heinemann, A. Scheurer, M. van Gastel, S. DeBeer, D. Munz and K. Meyer, *J. Am. Chem. Soc.*, 2023, **145**, 13650.

28 (*a*) S.-M. Au, J.-S. Huang, W.-Y. Yu, W.-H. Fung and C.-M. Che, *J. Am. Chem. Soc.*, 1999, **121**, 9120; (*b*) Y. Tokita, K. Yamaguchi, Y. Watanabe and I. Morishima, *Inorg. Chem.*, 1993, **32**, 329.